

Article

# A Numerical Solution of Fredholm Integral Equations of the Second Kind Based on Tight Framelets Generated by the Oblique Extension Principle

Mutaz Mohammad 

Department of Mathematics and Statistics, College of Natural and Health Sciences, Zayed University, Abu Dhabi 144543, UAE; Mutaz.Mohammad@zu.ac.ae; Tel.: +971-2-599-3496

Received: 22 May 2019; Accepted: 27 June 2019; Published: 2 July 2019



**Abstract:** In this paper, we present a new computational method for solving linear Fredholm integral equations of the second kind, which is based on the use of  $B$ -spline quasi-affine tight framelet systems generated by the unitary and oblique extension principles. We convert the integral equation to a system of linear equations. We provide an example of the construction of quasi-affine tight framelet systems. We also give some numerical evidence to illustrate our method. The numerical results confirm that the method is efficient, very effective and accurate.

**Keywords:** Fredholm integral equations; multiresolution analysis; unitary extension principle; oblique extension principle;  $B$ -splines; wavelets; tight framelets

## 1. Introduction

Integral equations describe many different events in science and engineering fields. They are used as mathematical models for many physical situations. Therefore, the study of integral equations and methods for solving them are very useful in application. The aim of this paper is to present a numerical method by using tight framelets for approximating the solution of a linear Fredholm integral equation of the second kind given by

$$u(x) = f(x) + \lambda \int_a^b \mathcal{K}(x,t)u(t)dt, \quad -\infty < a \leq x \leq b < \infty.$$

Although many numerical methods use wavelet expansions to solve integral equations, other types of methods work better with redundant systems, of which framelets are the easiest to use. The redundant system offered by frames has already been put to excellent use for many applications in science and engineering. Reference [1], particularly, frames play key roles in wavelet theory, time frequency analysis for signal processing, filter bank design in electrical engineering, the theory of shift-invariant spaces, sampling theory and many other areas (see e.g., References [2–7]). The concept of frame can be traced back to Reference [8]. It is known that the frame system is a redundant system. The redundancy of frames plays an important role in approximation analysis for many classes of functions. In the orthonormal wavelet systems, there is no redundancy. Hence, with redundant tight framelet systems, we have more freedom in building better reconstruction and approximation order.

Since 1991, wavelets have been applied in a wide range of applications and methods for solving integral equations. A short survey of these articles can be found in References [9,10]. There is a number of approximate methods for numerically solving various classes of integral equations [11,12]. It is known that Fredholm integral equations may be applied to boundary value problems and partial differential equations in practice. Also, there is a difficulty to find the analytic solution of Fredholm

integral equations. Here, we use a new and efficient method that generalizes the Galerkin-wavelet method used in the literature. We will call it the Galerkin-framelet method.

The paper is organized as follows. Section 2 is devoted to providing some preliminary background of frames, some notations and its function representation. Section 3 provides some fundamentals in the construction of quasi-affine  $B$ -spline tight framelet systems using the unitary extension principle and its generalization. We then begin the presentation of solving linear Fredholm integral equations based on the Galerkin-type method, based on quasi-affine tight framelets in Section 4. We present the error analysis of the proposed method in Section 5. We further present the numerical results and some graph illustrations in Section 6. We conclude with several remarks in Section 7.

## 2. Preliminary Results

Frame theory is a relatively emerging area in pure as well as applied mathematics research and approximation. It has been applied in a wide range of applications in signal processing [13], image denoising [14], and computational physics and biology [15]. Interested readers should consult the references therein to get a complete picture.

The expansion of a function in general is not unique. So, we can have a redundancy for a given representation. This happens, for instance, in the expansion using tight frames. Frames were introduced in 1952 by Duffin and Schaeffer [8]. They used frames as a tool in their paper to study a certain class of non-harmonic Fourier series. Thirty years later, Young introduced a beautiful development for abstract frames and presented their applications to non-harmonic Fourier series [16]. Daubechies et al. constructed frames for  $L^2(\mathbb{R})$  based on dilations and translation of functions [17]. These papers and others spurred a dramatic development of wavelet and framelet theory in the following years.

The space  $L^2(\mathbb{R})$  is the set of all functions  $f(x)$  such that

$$\|f\|_{L^2(\mathbb{R})} = \left( \int_{\mathbb{R}} |f(x)|^2 \right)^{1/2} < \infty.$$

**Definition 1.** A sequence  $\{f_k\}_{k=1}^{\infty}$  of elements in  $L^2(\mathbb{R})$  is a frame for  $L^2(\mathbb{R})$  if there exist constants  $A, B > 0$  such that

$$A\|f\|^2 \leq \sum_{k=1}^{\infty} |\langle f, f_k \rangle|^2 \leq B\|f\|^2, \forall f \in L^2(\mathbb{R}).$$

A frame is called tight if  $A = B$ .

Let  $\ell_2(\mathbb{Z})$  be the set of all sequences of the form  $h[k]$  defined on  $\mathbb{Z}$ , satisfying

$$\left( \sum_{k=-\infty}^{\infty} |h[k]|^2 \right)^{1/2} < \infty.$$

The Fourier transform of a function  $f \in L^2(\mathbb{R})$  is defined by

$$\widehat{f}(\xi) = \int_{\mathbb{R}} f(t) e^{-i\xi t} dt, \xi \in \mathbb{R},$$

and its inverse is

$$f(x) = \frac{1}{2\pi} \int_{\mathbb{R}} \widehat{f}(\xi) e^{i\xi x} d\xi, x \in \mathbb{R}.$$

Similarly, we can define the Fourier series for a sequence  $h \in \ell_2(\mathbb{Z})$  by

$$\widehat{h}(\xi) = \sum_{k \in \mathbb{Z}} h[k] e^{-i\xi k}.$$

**Definition 2.** A compactly supported function  $\phi \in L^2(\mathbb{R})$  is said to be refinable if

$$\phi(x) = 2 \sum_{k \in \mathbb{Z}} h_0[k] \phi(2x - k), \tag{1}$$

for some finite supported sequence  $h_0[k] \in \ell_2(\mathbb{Z})$ . The sequence  $h_0$  is called the low pass filter of  $\phi$ .

A wavelet is said to have a vanishing moment of order  $m$  if

$$\int_{-\infty}^{\infty} x^p \psi(x) dx = 0; \quad p = 0, \dots, m - 1.$$

To formulate the matrix form and the numerical solution of a given Fredholm integral equation, we will study and use tight framelets and their constructions that are derived from the unitary extension principle (UEP) and the oblique extension principle (OEP) [18]. The UEP is a method to construct tight frame wavelet filters. We recall a result by Ron and Shen, Theorem 1, which constructs a tight frame from the UEP generated by a collection  $\{\psi^\ell\}_{\ell=1}^r$ . The interested reader may consult References [19–21], and other related references for more details.

Let  $\Psi = \{\psi^\ell\}_{\ell=1}^r \subset L^2(\mathbb{R})$  be of the form

$$\psi^\ell = 2 \sum_{k \in \mathbb{Z}} h_\ell[k] \phi(2 \cdot -k), \tag{2}$$

where  $\{h_\ell[k], k \in \mathbb{Z}\}_{\ell=1}^r$  is a finitely supported sequence and is called the high pass filter of the system.

**Theorem 1** (Unitary Extension Principle [20]). Let  $\phi \in L^2(\mathbb{R})$  be the compactly supported refinable function with its finitely supported low pass filter  $h_0$ . Let  $\{h_\ell[k], k \in \mathbb{Z}, \ell = 1, \dots, r\}$  be a set of finitely supported sequences, then the system

$$X(\Psi) = \{\psi_{j,k}^\ell : 1 \leq \ell \leq r ; j, k \in \mathbb{Z}\}, \tag{3}$$

where  $\psi_{j,k}^\ell = 2^{j/2} \psi^\ell(2^j x - k)$ , forms a tight frame for  $L^2(\mathbb{R})$  provided the equalities

$$\sum_{\ell=0}^r |\widehat{h}_\ell(\xi)|^2 = 1 \quad \text{and} \quad \sum_{\ell=0}^r \widehat{h}_\ell(\xi) \widehat{h}_\ell(\xi + \pi) = 0 \tag{4}$$

hold for all  $\xi \in [-\pi, \pi]$ .

For the proof see [18].

This means for any  $f \in L^2(\mathbb{R})$ , we have the following tight framelets representation,

$$f = \sum_{\ell=1}^r \sum_{j \in \mathbb{Z}} \sum_{k \in \mathbb{Z}} \langle f, \psi_{j,k}^\ell \rangle \psi_{j,k}^\ell. \tag{5}$$

The representation (5) is one of many; however, it is known as the best possible representation of  $f$ , which can be truncated by  $S_n$ , where

$$S_n f = \sum_{\ell=1}^r \sum_{j < n} \sum_{k \in \mathbb{Z}} \langle f, \psi_{j,k}^\ell \rangle \psi_{j,k}^\ell, \quad n \in \mathbb{N}, \tag{6}$$

which are known as the quasi-projection operators [4].

Note that  $S_n f \in L^2(\mathbb{R})$  and  $\lim \|S_n f - f\|_2 = 0$  as  $n \rightarrow \infty$  [22]. We will use this representation to find the numerical solutions of a given Fredholm integral equation using the quasi-affine tight framelets generated by some refinable functions.

### 3. Quasi-Affine B-Spline Tight Framelet Systems

There is an interesting family of refinable functions known as  $B$ -splines. It has an important role in applied mathematics, geometric modeling and many other areas [23,24]. An investigation of the frame set using a class of functions that called generalized  $B$ -spline and which includes the  $B$ -spline has been studied extensively in Reference [25].

In applications, the  $B$ -splines of order 2 and 4 are more popular than those of other orders. Also, it is preferred to have the  $B$ -splines to be centered at  $x = 0$ . Therefore, we define the centered  $B$ -splines as follows:

**Definition 3** ([26]). The  $B$ -spline  $B_{m+1}$  is defined as follows by using the convolution

$$B_{m+1}(x) := (B_m * B_1)(x), x \in \mathbb{R},$$

where  $B_1(x)$  is defined to be  $\chi_{[-\frac{1}{2}, \frac{1}{2}]}(x)$ , the characteristic function for the interval  $[-\frac{1}{2}, \frac{1}{2}]$ .

Figure 1 shows the graphs of the first few  $B$ -splines.

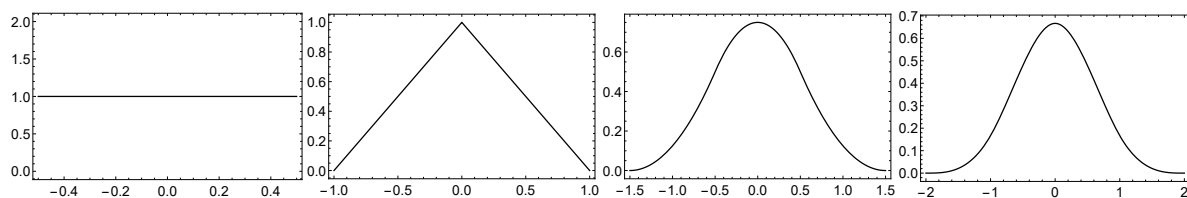


Figure 1. The  $B$ -splines  $B_m$  for  $m = 1, \dots, 4$ , respectively.

One can easily show that the Fourier transform of the  $B$ -spline,  $B_m$ , of order  $m$  is given by

$$\widehat{B}_m(\xi) = e^{-i\xi d} \left( \frac{\sin(\xi/2)}{\xi/2} \right)^m \quad \text{and} \quad \widehat{h}_0^m(\xi) = e^{-i\xi d/2} \cos^m(\xi/2),$$

where  $d = 0$  if  $m$  is even, and  $d = 1$  if  $m$  is odd. We refer to [27] for more details.

#### 3.1. Framelets by the UEP and Its Generalization

The UEP is a method to construct tight framelets from a given refinable function. For a given refinable function and to construct tight framelets system, the function  $\Theta$ , which is non-negative, essentially bounded and continuous at the origin with  $\Theta(0) = 1$ , should satisfy the following conditions

$$\begin{cases} \Theta(2\xi)|\widehat{h}_0(\xi)|^2 + \sum_{\ell=1}^r |\widehat{h}_\ell(\xi)|^2 = \Theta(\xi); \\ \Theta(2\xi)\widehat{h}_0(\xi)\widehat{h}_0(\xi + \pi) + \sum_{\ell=1}^r \widehat{h}_\ell(\xi)\widehat{h}_\ell(\xi + \pi) = 0. \end{cases} \quad (7)$$

In applications, it is recommended to use tight framelet systems that are shift-invariant. The set of functions is said to be  $\rho$ -shift-invariant if for any  $k \in \mathbb{Z}$  and  $\psi \in \mathcal{S}$ , we have  $\psi(\cdot - \rho k) \in \mathcal{S}$ . Hence, the quasi-affine system was introduced to convert the system  $X(\Psi)$  (not shift-invariant) to a shift-invariant system. Next, we present a quasi-affine system that allows us to construct a quasi-affine tight framelet. This system is not an orthonormal basis [28].

**Definition 4** ([22]). Let  $\Psi$  be defined as in the UEP. A corresponding quasi-affine system from level  $J$  is defined as

$$X^J(\Psi) = \left\{ \psi_{j,k}^\ell : 1 \leq \ell \leq r, j, k \in \mathbb{Z}, \right\}$$

where  $\psi_{j,k}^\ell$  is given by

$$\psi_{j,k}^\ell = \begin{cases} 2^{j/2} \psi^\ell(2^j \cdot -k), & j \geq J \\ 2^j \psi^\ell(2^j (\cdot - 2^{-j}k)), & j < J \end{cases} .$$

The quasi-affine system is created by changing the basic definition of  $\psi_{j,k}^\ell$  by sampling the tight framelet system from the level  $J - 1$  and below. Therefore, the system  $X^J(\Psi)$  is a  $2^{-J}$ -shift-invariant system. Note that this downward sampling in the definition will not change the approximation order as it is the same for both systems. So the error analysis will be the same. We use this definition to solve a given Fredholm integral equation that will be defined later in Section 4. In the study of our expansion method, we consider  $J = 0$  where  $X^0(\Psi)$  generates a quasi-affine tight framelet system for  $L^2(\mathbb{R})$  but not an orthonormal basis as stated earlier. It is well known that the system  $X^J(\Psi)$  is a tight framelet  $L^2(\mathbb{R})$  iff  $X(\Psi)$  it is a tight framelet for  $L^2(\mathbb{R})$ . We refer the reader to Reference [22] for full details of the relation and analysis of both affine and quasi-affine systems.

To construct quasi-affine tight framelets generated by the OEP, (see Reference [20]), we should choose  $\Theta$  as a suitable approximation at  $\xi = 0$  to the fraction  $1/|\widehat{\phi}|$ . As an example for the  $B$ -spline of order  $m$ , we should choose  $\Theta$  to be a  $2\pi$ -periodic function that approximates the reciprocal of

$$\left| \frac{\sin(\xi/2)}{\xi/2} \right|^{2m}$$

at  $\xi = 0$ .

If  $\widehat{h}_0$  is the low pass filter of a refinable function, then based on the OEP and to construct quasi-affine tight framelets, it is assumed [22] that

$$H(\xi) = \Theta(\xi) - \Theta(2\xi)|\widehat{h}_0(\xi)|^2 - \Theta(2\xi)|\widehat{h}_0(\xi + \pi)|^2 \geq 0. \tag{8}$$

This condition will help to find high pass filters easily. Let  $|h|^2 = H$  and  $|\theta|^2 = \Theta$ . Here the square root is obtained by the Féjer-Riesz lemma [2]. Choose  $c_2, c_3$  to be  $2\pi$ -periodic trigonometric polynomials such that

$$|c_2(\xi)|^2 + |c_3(\xi)|^2 = 1, \quad c_2(\xi)\overline{c_2(\xi + \pi)} + c_3(\xi)\overline{c_3(\xi + \pi)} = 0.$$

Then, we can find three high pass filters, namely

$$\widehat{h}_1(\xi) = e^{i\xi\theta(2\xi)} \overline{\widehat{h}_0(\xi + \pi)}, \quad \widehat{h}_2(\xi) = c_2(\xi)h(\xi), \quad \widehat{h}_3(\xi) = c_3(\xi)h(\xi),$$

with a standard choice of  $c_2(\xi) = (1/\sqrt{2})$ , and  $c_3(\xi) = (1/\sqrt{2})e^{i\xi}$ .

If we consider the UEP rather than the OEP in the construction above, that is,  $\Theta = 1$ , then we will use the assumption that

$$|\widehat{h}_0(\xi)|^2 + |\widehat{h}_0(\xi + \pi)|^2 \leq 1.$$

Define the high pass filters as

$$\widehat{h}_1(\xi) = e^{i\xi} \overline{\widehat{h}_0(\pi + \xi)}, \quad \widehat{h}_2(\xi) = (\sqrt{2}/2)h(\xi), \quad \widehat{h}_3(\xi) = e^{i\xi} \widehat{h}_2(\xi).$$

The number of generators can be reduced from three to two with the new fundamental function  $1 - H$ , where

$$\widehat{h}_1(\xi) = e^{i\xi\theta(2\xi)} \overline{\widehat{h}_0(\pi + \xi)}, \quad \widehat{h}_2(\xi) = h_0(\xi)h(2\xi). \tag{9}$$

However, this usually will affect the generators system by having less symmetry of the generators or longer filters.

### 3.2. Examples of Quasi-Affine B-Spline Tight Framelets

Next, we give some examples of quasi-affine B-spline tight framelets of  $L^2(\mathbb{R})$  constructed via the UEP (OEP).

**Example 1** (Quasi-affine HAAR framelet (HAAR framelet)). Let  $h_0 = [\frac{1}{2}, \frac{1}{2}]$  be the low pass filter of  $B_1(x)$ . By Equations (4), we have  $h_1[k] = [\frac{1}{2}, -\frac{1}{2}]$ . Then, the system  $X^0(\psi_1)$  forms a quasi-affine tight framelet system for  $L^2(\mathbb{R})$ .

**Example 2** ( $B_2$ -UEP). Let  $h_0 = [\frac{1}{4}, \frac{1}{2}, \frac{1}{4}]$  be the low pass filter of  $B_2(x)$ . We used Mathematica to obtain the high pass filters  $h_1$  and  $h_2$ , namely,  $h_1 = \pm[-\frac{1}{4}, \frac{1}{2}, -\frac{1}{4}]$ ;  $h_2 = \pm[-\frac{\sqrt{2}}{4}, 0, \frac{\sqrt{2}}{4}]$ . Considering Theorem 1, we obtain that the system  $X^0(\{\psi_\ell\}_{\ell=1}^2)$  forms a quasi-affine tight framelet system for  $L^2(\mathbb{R})$ .  $B_2$  and its quasi-affine tight framelet generators  $\psi_1, \psi_2$  are illustrated in Figure 2.

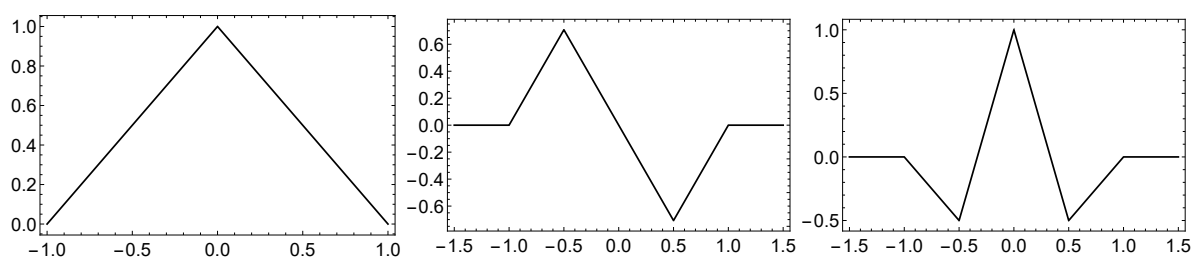


Figure 2. Piecewise linear B-spline,  $B_2(x)$ , and the corresponding tight framelets.

**Example 3** ( $B_4$ -UEP). Let  $h_0 = [\frac{1}{16}, \frac{1}{4}, \frac{3}{8}, \frac{1}{4}, \frac{1}{16}]$  be the low pass filter of  $B_4(x)$ . Define

$$\begin{cases} h_1 = [\frac{1}{16}, -\frac{1}{4}, \frac{3}{8}, -\frac{1}{4}, \frac{1}{16}], & h_2 = [\frac{1}{8}, -\frac{1}{4}, 0, \frac{1}{4}, -\frac{1}{8}], \\ h_3 = [\frac{1}{8}\sqrt{\frac{3}{2}}, 0, -\frac{1}{4}\sqrt{\frac{3}{2}}, 0, \frac{1}{8}\sqrt{\frac{3}{2}}], & h_4 = [-\frac{1}{8}, -\frac{1}{4}, 0, \frac{1}{4}, \frac{1}{8}]. \end{cases}$$

Then,  $h_0, h_1$  and  $h_2$  satisfy Equation (4). Hence, the system  $X^0(\Psi)$  is a quasi-affine tight framelet system for  $L^2(\mathbb{R})$ . The cubic quasi-affine tight framelets functions,  $\psi_1, \psi_2, \psi_3$ , and  $\psi_4$ , are depicted in Figure 3.

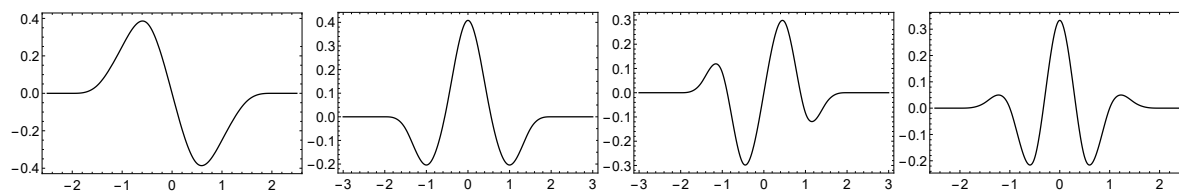


Figure 3. The corresponding tight framelets generated by the cubic B-spline.

Let us illustrate the discussion by providing some examples of quasi-affine tight framelets generated using the OEP.

**Example 4** ( $B_2$ -OEP). Consider the hat function, the linear B-spline  $B_2$ , and  $\Theta(\zeta) = 4/3 - e^{-i\zeta}/6 - e^{i\zeta}/6$ . Define  $\Psi = \{\psi_1, \psi_2\}$ , where

$$\widehat{\psi}_1(\zeta) = \frac{-1}{\zeta^2} \left(1 - e^{-i\zeta/2}\right)^4 \quad \text{and} \quad \widehat{\psi}_2(\zeta) = \frac{1}{\sqrt{6}\zeta^2} \left(-1 + e^{-i\zeta/2}\right)^4 \left(1 + 4e^{-i\zeta/2} + e^{-i\zeta}\right).$$

where  $\theta$  and  $h$  in Equation (9) are obtained by using the spectral factorization theorem in [2]. Note that in time domain, we have

$$\psi_1(x) = |1 - 2x| + |3 - 2x| - \frac{1}{2}|-2 + x| - 3|-1 + x| - \frac{1}{2}|x|, \text{ and}$$

$$\psi_2(x) = \frac{1}{\sqrt{6}} \left( -4|3 - 2x| + \frac{1}{2}|-3 + x| - \frac{9}{2}|-2 + x| + \frac{1}{2}|-1 + x| + \frac{1}{2}|x| \right),$$

Then, the system  $X(\Psi)$  generated using Equation (7) forms a quasi-affine tight framelet system for  $L^2(\mathbb{R})$ .  $B_2$ , and its quasi-affine tight framelets,  $\psi_1, \psi_2$ , are given in Figure 4.

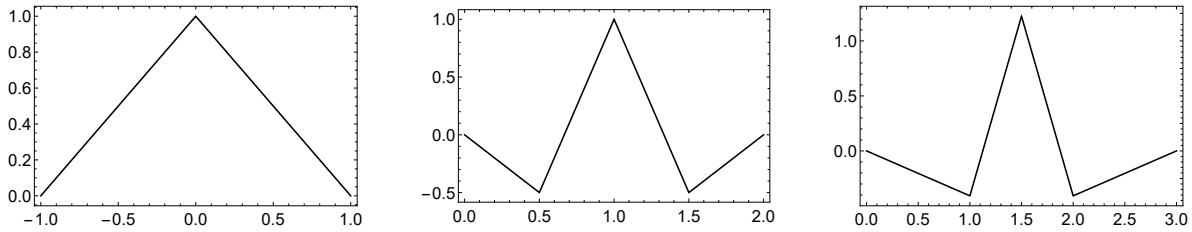


Figure 4. Piecewise linear B-spline,  $B_2(x)$ , and the corresponding quasi-affine tight framelets generated by the oblique extension principle (OEP).

**Example 5 ( $B_4$ -OEP).** Consider  $B_4(x)$ , the cubic B-spline, and take the periodic function  $\Theta$  defined by

$$\Theta(\xi) = 2.59471 - 0.98631e^{-i\xi} - 0.98631e^{i\xi} + 0.209524e^{-2i\xi} + 0.209524e^{2i\xi} - 0.0205688e^{-3i\xi} - 0.0205688e^{3i\xi}.$$

Now, define  $\Psi$ , where  $r = 3$ , as follows

$$\psi_1(x) = 0.252839|3 - 2x|^3 + 0.707948|5 - 2x|^3 + 0.252839|7 - 2x|^3 + 0.0126419|-5 + x|^3 - 0.442468|-4 + x|^3 - 4.42468|-3 + x|^3 - 4.42468|-2 + x|^3 - 0.442468|1 + x|^3 + 0.0126419|x|^3,$$

$$\psi_2(x) = -0.07207963|3 - 2x|^3 - 1.21209103|5 - 2x|^3 - 1.21209103|7 - 2x|^3 - 0.07207963|9 - 2x|^3 + 0.01105521|-6 + x|^3 - 0.08269335|-5 + x|^3 + 3.95289189|-4 + x|^3 + 12.78422305|-3 + x|^3 + 3.95289189|-2 + x|^3 - 0.08269335|-1 + x|^3 + 0.01105521|x|^3,$$

$$\psi_3(x) = 0.0666740|5 - 2x|^3 + 0.798605|7 - 2x|^3 + 0.0666740|9 - 2x|^3 - 2.12302 \times 10^{-17}|11 - 2x|^3 + 0.0119515|-7 + x|^3 - 0.113791|-6 + x|^3 + 0.468945|-5 + x|^3 - 4.09492|-4 + x|^3 - 4.09492|-3 + x|^3 + 0.468945|-2 + x|^3 - 0.113791|-1 + x|^3 + 0.0119515|x|^3.$$

Then, the system  $X^0(\Psi)$  satisfy Equation (7) and then forms a quasi-affine tight framelet system for  $L^2(\mathbb{R})$ . The cubic B-spline,  $B_4$ , and its quasi-affine tight framelet generators  $\psi_1, \psi_2, \psi_3$  are given in Figure 5.

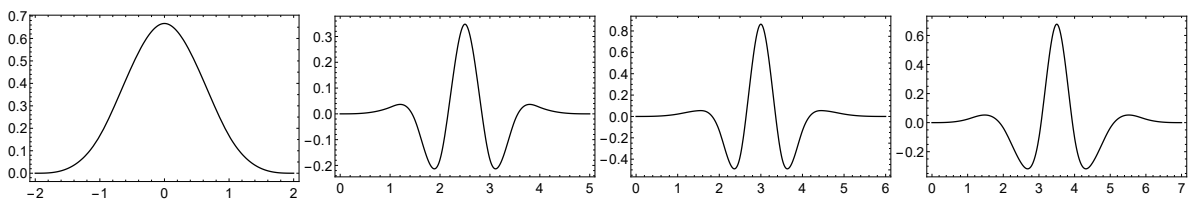


Figure 5. The B-spline  $B_4(x)$  and the corresponding tight framelets generated by the OEP.

The function  $H$  in Equation (8) for the  $B$ -splines of order 2 and 4 are illustrated in Figure 6. Note that for  $B_2$ , we have

$$H(\zeta) = \frac{1}{48} \left( 64 - 16 \Re(e^{-i\zeta}) - 4 \left( |1 + e^{-i\zeta}|^4 + |1 - e^{i\zeta}|^4 \right) + \Re(e^{-2i\zeta}) \left( |1 + e^{-i\zeta}|^4 + |1 - e^{i\zeta}|^4 \right) \right).$$

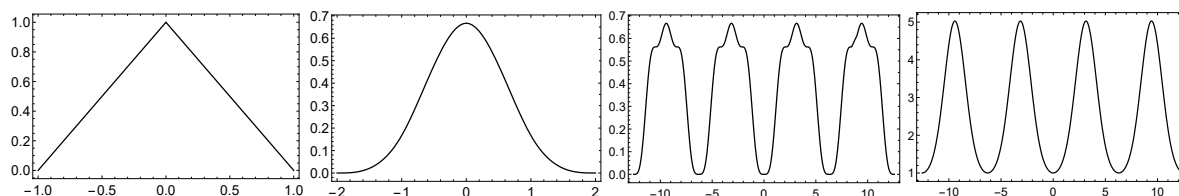


Figure 6. Illustration of  $B_2$  and  $B_4$ , with its corresponding positive function  $H$ , respectively.

### 4. Solving Fredholm Integral Equation via Tight Framelets

Many methods have been presented to find exact and approximate solutions of different integral equations. In this work, we introduce a new method for solving the above-mentioned class of equations. We use quasi-affine tight framelets systems generated by the UEP and OEP for solving some types of integral equations. Consider the second-kind linear Fredholm integral equation of the form:

$$u(x) = f(x) + \lambda \int_a^b \mathcal{K}(x,t)u(t)dt, \quad -\infty < a \leq x \leq b < \infty, \tag{10}$$

where  $\lambda$  is a real number,  $f$  and  $\mathcal{K}$  are given functions and  $u$  is an unknown function to be determined.  $\mathcal{K}$  is called the kernel of the integral Equation (10). A function  $u(x)$  defined over  $[a, b]$  can be expressed by quasi-affine tight framelets as Equation (5). To find an approximate solution  $u_n$  of (10), we will truncate the quasi-affine framelet representation of  $u$  as in Equation (6). Then,

$$u(x) \approx u_n(x) = \sum_{\ell=1}^r \sum_{j < n} \sum_{k \in \mathbb{Z}} c_{j,k}^\ell \psi_{j,k}^\ell(x), \tag{11}$$

where

$$c_{j,k}^\ell = \int_{\mathbb{R}} u_n(x) \psi_{j,k}^\ell(x) dx.$$

Substituting (11) into (10) yields

$$\sum_{\ell=1}^r \sum_{j < n} \sum_{k \in \mathbb{Z}} c_{j,k}^\ell \psi_{j,k}^\ell(x) = f(x) + \lambda \sum_{\ell=1}^r \sum_{j < n} \sum_{k \in \mathbb{Z}} c_{j,k}^\ell \int_a^b \mathcal{K}(x,t) \psi_{j,k}^\ell(t) dt \tag{12}$$

Multiply Equation (12) by  $\sum_{s=1}^r \psi_{p,q}^s(x)$  and integrate both sides from  $a$  to  $b$ . This can be a generalization of Galerkin method used in Reference [29,30]. Then, with a few algebra, Equation (12) can be simplified to a system of linear equations with the unknown coefficients  $c_{j,k}^\ell$  (to be determined) given by

$$\sum_{s,\ell=1}^r \sum_{j < n} \sum_{k \in \mathbb{Z}} c_{j,k}^\ell m_{j,k,p,q}^{\ell,s} = g_{p,q}, \quad p, q \in \mathbb{Z}, \tag{13}$$

where

$$m_{j,k,p,q}^{\ell,s} = \int_a^b \psi_{j,k}^\ell(x) \psi_{p,q}^s(x) dx - \lambda \int_a^b \int_a^b \mathcal{K}(x,t) \psi_{j,k}^\ell(t) \psi_{p,q}^s(x) dx dt, \quad p, q \in \mathbb{Z}$$

and

$$g_{p,q} = \sum_{s=1}^r \int_a^b f(x) \psi_{p,q}^s(x) dx, \quad p, q \in \mathbb{Z}. \tag{14}$$

Note that, evaluating the values in Equation (14) and by considering the Haar framelet system, we are able to determine the values of  $j, k$  for which the representation in Equation (11) is accurate. This is done by avoiding the inner products that have zero values. If interval is  $[0, 1]$  and  $j = -n, \dots, n$ , then  $k = -2^n, \dots, 2^n - 1$ . Thus, we have a linear system of order  $2^{n+1}(2n + 1)$  to be solved. This system can be reduced to a smaller order by ignoring those zero inner products and again that depends on the framelet's support and the function domain being handled. Now the unknown coefficients are determined by solving the resulting system of Equation (13), and then we get the approximate solution  $u_n$  in Equation (11).

This can be formulated as a matrix form

$$M^T C = G,$$

where, for example, in the case of quasi-affine Haar framelet system, if

$$j = -n, \dots, a, \dots, n; \quad p = -n, \dots, \alpha, \dots, n; \quad k = -2^n, \dots, b, \dots, 2^n - 1; \quad q = -2^n, \dots, \beta, \dots, 2^n - 1; \\ \ell = 1, \dots, x, \dots, r; \quad \text{and } s = 1, \dots, d, \dots, r,$$

then, the matrix  $M$  and the column vectors  $C$  and  $G$  are given by

$$M = \begin{pmatrix} m_{-n,-2^n,-n,-2^n}^{1,1} & \cdots & m_{a,b,-n,-2^n}^{x,d} & \cdots & m_{n,2^n-1,-n,-2^n}^{r,r} \\ \vdots & \ddots & \vdots & \ddots & \vdots \\ m_{-n,-2^n,\alpha,\beta}^{1,1} & \vdots & m_{a,b,\alpha,\beta}^{x,d} & \vdots & m_{n,2^n-1,\alpha,\beta}^{r,r} \\ \vdots & \ddots & \vdots & \ddots & \vdots \\ m_{-n,-2^n,n,2^n-1}^{1,1} & \cdots & m_{a,b,n,2^n-1}^{x,d} & \cdots & m_{n,2^n-1,n,2^n-1}^{r,r} \end{pmatrix}$$

$$C = [c_{-n,-2^n}^1, \dots, c_{a,b}^x, \dots, c_{n,2^n-1}^r], \\ G = [g_{-n,-2^n}, \dots, g_{a,b}, \dots, g_{n,2^n-1}].$$

such that  $C$  and  $G$  are  $2^{n+1}(2n + 1) \times 1$  column vectors, and  $M$  is an  $2^{n+1}(2n + 1) \times 2^{n+1}(2n + 1)$  matrix. The absolute error for this formulation is defined by

$$e_n = \|u(x) - u_n(x)\|_2, \quad x \in [a, b].$$

The error function is defined to be

$$E_n(x) = |u(x) - u_n(x)|, \quad x \in [a, b].$$

### 5. Error Analysis

In this section, we get an upper bound for the error of our method. Let  $\phi$  be as in Equation (1) and  $W_2^m(\mathbb{R})$  is the Sobolev space consists of all square integrable functions  $f$  such that  $\{f^{(k)}\}_{k=0}^m \in L^2(\mathbb{R})$ . Then,  $X^0(\Psi)$  provides approximation order  $m$ , if

$$\|f - S_n f\|_2 \leq C 2^{-nm} \|f^{(m)}\|_2, \quad \forall f \in W_2^m(\mathbb{R}), n \in \mathbb{N}.$$

The approximation order of the truncated function  $S_n$  was studied in References [20,31]. It is well known in the literature that the vanishing moments of the framelets can be determined by its low and high pass filters  $\hat{h}_\ell, \ell = 0, \dots, r$ . Also, if the quasi-affine framelet system has vanishing moments of order say  $m_1$  and the low pass filter of the system satisfy the following,

$$1 - |\hat{h}_0(\xi)|^2 = \mathcal{O}(|\cdot|^{2m}),$$

at the origin, then the approximation order of  $X^0(\Psi)$  is equal to  $\min\{m_1, m\}$ . Therefore, as the OEP increases the vanishing moments of the quasi-affine framelet system, the accuracy order of the truncated framelet representation, will increase as well.

As mentioned earlier, integral equations describe many different events in applications such as image processing and data reconstructions, for which the regularity of the function  $f$  is low and does not meet the required order of smoothness. This makes the determination of the approximation order difficult from the functional analysis side. Instead, it is assumed that the solution function to satisfy a decay condition with a wavelet characterization of Besov space  $B_{2,2}^s$ . We refer the reader to Reference [32] for more details. Hence, we impose the following decay condition such that

$$N_f = \sum_{\ell=1}^r \sum_{j \geq 0} \sum_{k \in \mathbb{Z}} 2^{sj} |\langle f, \psi_{j,k}^\ell \rangle| < \infty, \quad (15)$$

where  $s \geq -1$ .

**Theorem 2.** Let  $X^0(\Psi)$  be a quasi-tight framelet system generated using the OEP from the compactly supported function  $\phi$ . Assume that  $f$  satisfies the condition (15). Then,

$$\|f - S_n f\|_2 \leq N_f \mathcal{O}(2^{-(s+1)n}). \quad (16)$$

**Proof.** Using Bessel property of  $X(\Psi)$ , and by Equation (6), we have

$$\begin{aligned} \|f - S_n f\|_2^2 &= \left\| \sum_{\ell=1}^r \sum_{j \geq n} \sum_{k \in \mathbb{Z}} \langle f, \psi_{j,k}^\ell \rangle \psi_{j,k}^\ell \right\|_2^2 \\ &\leq \sum_{\ell=1}^r \sum_{j \geq n} \sum_{k \in \mathbb{Z}} |\langle f, \psi_{j,k}^\ell \rangle|^2. \end{aligned}$$

Note that

$$|\langle f, \psi_{j,k}^\ell \rangle| \leq \|f\|_\infty \|\psi_{j,k}^\ell\|_1 = \|f\|_\infty 2^{-j/2} \|\psi^\ell\|_1.$$

This leads to the following

$$\begin{aligned} \|f - S_n f\|_2^2 &\leq \|f\|_\infty \max_{\ell} \|\psi^\ell\|_1 \sum_{\ell=1}^r \sum_{j \geq n} \sum_{k \in \mathbb{Z}} 2^{-j} |\langle f, \psi_{j,k}^\ell \rangle| \\ &\leq \|f\|_\infty \max_{\ell} \|\psi^\ell\|_1 \sum_{\ell=1}^r \sum_{j \geq n} \sum_{k \in \mathbb{Z}} 2^{-j} \frac{2^{j(s+1)}}{2^{n(s+1)}} |\langle f, \psi_{j,k}^\ell \rangle| \\ &\leq \|f\|_\infty \max_{\ell} \|\psi^\ell\|_1 2^{-(s+1)n} N_f. \end{aligned}$$

Thus, the inequality (16) is concluded.  $\square$

## 6. Numerical Performance and Illustrative Examples

Based on the method presented in this paper, we solve the following examples using the quasi-affine tight framelets constructed in Section 3.2. The computations associated with these examples were obtained using Mathematica software.

**Example 6.** We consider the Fredholm integral equation of 2nd kind defined by:

$$u(x) = 1 + \int_{-1}^1 (xt + x^2 t^2) u(t) dt.$$

The exact solution is  $u(x) = 1 + \frac{10}{9}x^2$ .

In Tables 1 and 2 the absolute error  $e_n$  for different values of  $n$  and the numerical values of  $u_n(x)$  when  $n = 2$  are computed, respectively. Using quasi-affine Haar framelet system, Figures 7 and 8 demonstrated the graphs of the exact and approximate solutions and Figure 9 demonstrated the graphs of  $E_n(x)$  for different values of  $n$ . For the case of  $B_2$ -UEP, Figure 10 demonstrated the graphs of the exact and approximate solutions for different values of  $n$ .

**Table 1.** The errors  $e_n$  of Example 6 for five different quasi-affine tight framelet systems generated by the unitary extension principle (UEP) and OEP, for increasing  $n$ .

$n$	HAAR Framelet	$B_2$ -UEP	$B_4$ -UEP	$B_2$ -OEP	$B_4$ -OEP
2	$6.55 \times 10^{-2}$	$1.83 \times 10^{-3}$	$8.89 \times 10^{-6}$	$1.82 \times 10^{-3}$	$8.24 \times 10^{-6}$
3	$3.27 \times 10^{-2}$	$4.58 \times 10^{-4}$	$9.09 \times 10^{-6}$	$6.78 \times 10^{-4}$	$1.43 \times 10^{-7}$
4	$1.64 \times 10^{-2}$	$1.14 \times 10^{-4}$	$1.39 \times 10^{-7}$	$3.25 \times 10^{-4}$	$9.46 \times 10^{-7}$
5	$8.18 \times 10^{-3}$	$2.86 \times 10^{-5}$	$2.45 \times 10^{-8}$	$1.87 \times 10^{-5}$	$1.03 \times 10^{-9}$
6	$4.09 \times 10^{-3}$	$7.15 \times 10^{-5}$	$1.33 \times 10^{-8}$	$7.01 \times 10^{-6}$	$5.71 \times 10^{-10}$
7	$1.77 \times 10^{-4}$	$9.88 \times 10^{-6}$	$9.33 \times 10^{-9}$	$8.79 \times 10^{-6}$	$9.42 \times 10^{-11}$
8	$5.92 \times 10^{-4}$	$5.73 \times 10^{-6}$	$7.40 \times 10^{-10}$	$3.08 \times 10^{-7}$	$5.08 \times 10^{-12}$
9	$1.70 \times 10^{-5}$	$4.03 \times 10^{-7}$	$4.22 \times 10^{-11}$	$4.01 \times 10^{-8}$	$3.32 \times 10^{-13}$
10	$8.65 \times 10^{-5}$	$1.21 \times 10^{-8}$	$3.52 \times 10^{-12}$	$1.32 \times 10^{-9}$	$2.21 \times 10^{-13}$

**Table 2.** Numerical results of the function  $u_n$  of Example 6 using different quasi-affine tight framelets and for a level of  $n = 2$ .

$x$	Exact	HAAR Framelet	$B_2$ -UEP	$B_4$ -UEP	$B_2$ -OEP	$B_4$ -OEP
-0.9	1.9000000	1.9723995	1.8998802	1.8999970	1.8998802	1.9000001
-0.7	1.5444444	1.5235997	1.5457151	1.5444398	1.5457151	1.5444444
-0.5	1.2777777	1.2128922	1.2748830	1.2777713	1.2748830	1.2777777
-0.3	1.1000000	1.1093230	1.1012727	1.0999958	1.1012727	1.1000000
-0.1	1.0111111	1.0057538	1.0109953	1.0111080	1.0109953	1.0111100
0.0	1.0000000	1.0001228	0.9971065	0.9999965	0.9971065	1.0000000
0.1	1.0111111	1.0057538	1.0109953	1.0111078	1.0109953	1.0111110
0.3	1.1000000	1.1093230	1.1012727	1.0999938	1.1012727	1.1000000
0.5	1.2777777	1.3509844	1.2748830	1.2777699	1.2748830	1.2777777
0.7	1.5444444	1.5235997	1.5457151	1.5444346	1.5457151	1.5444442
0.9	1.9000000	1.9723995	1.8998802	1.8999885	1.8998802	1.9000000

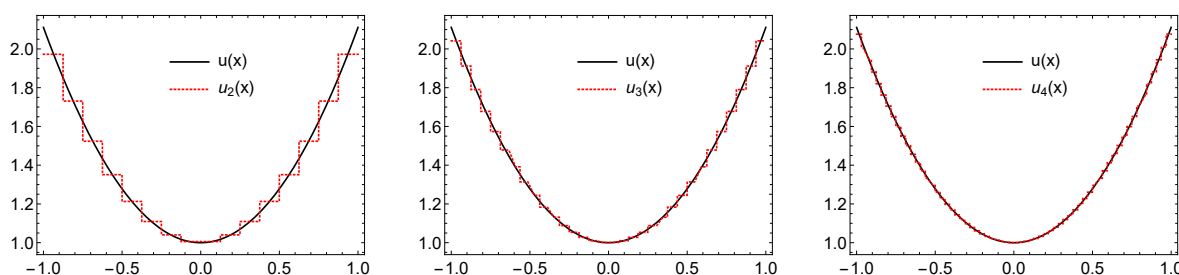


**Figure 7.** The graphs of  $u$  and  $u_n$  for  $n = 2, 3, 4$ , respectively, based on the quasi-affine HAAR framelet system of Example 6.

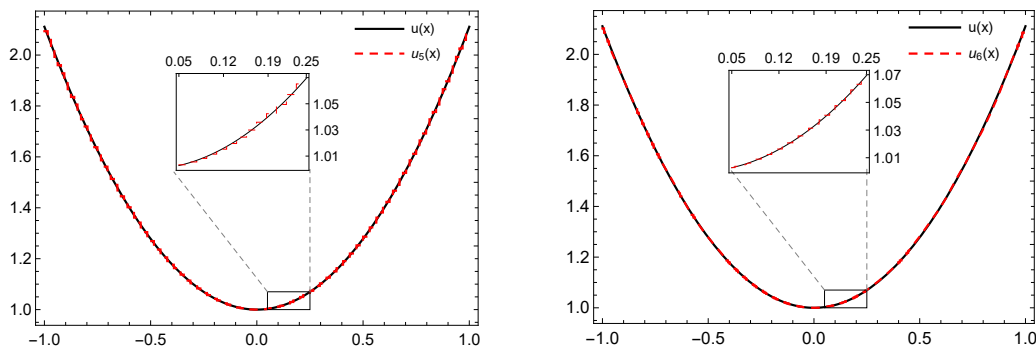


Figure 8. The graphs of  $u$  and  $u_n$  for  $n = 5, 6$ , respectively, based on the quasi-affine HAAR framelet system of Example 6.

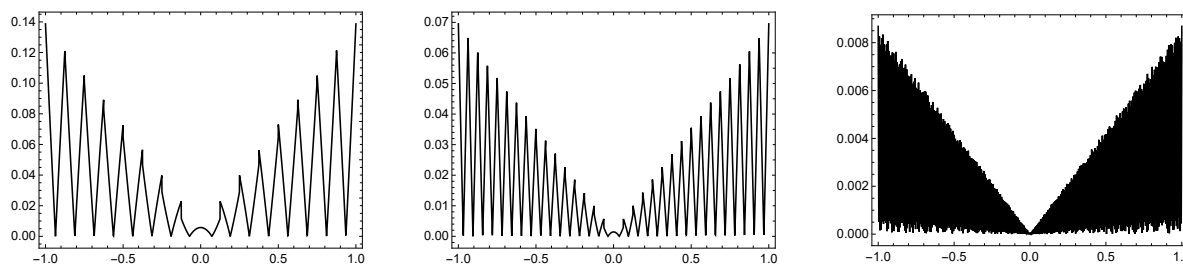


Figure 9. The graphs of  $E_n(x)$  for  $n = 2, 3, 6$ , respectively, and based on quasi-affine HAAR framelet system of Example 6.

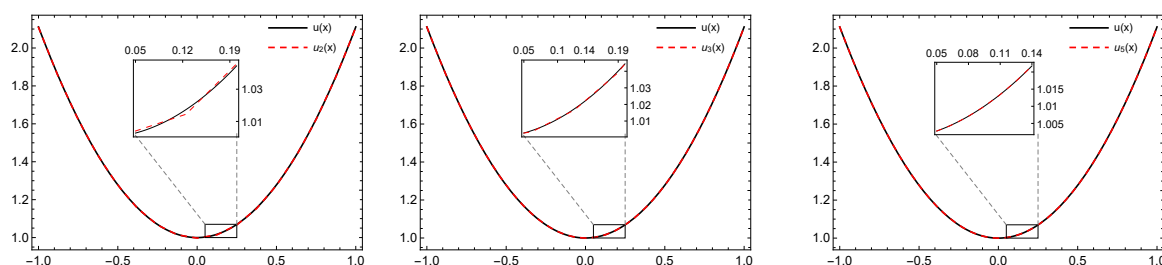


Figure 10. The graphs of  $u$  and  $u_n$  for  $n = 2, 3, 5$ , respectively, based on the quasi-affine  $B_2$ -UEP framelet system.

Example 7. We consider the Fredholm integral equation of 2nd kind defined by:

$$u(x) = e^x - \frac{e^{x+1} - 1}{x + 1} + \int_0^1 e^{xt} u(t) dt.$$

The exact solution is  $u(x) = e^x$ .

In Tables 3 and 4 the absolute error  $e_n$  for different values of  $n$  and the numerical values of  $u_n(x)$  when  $n = 2$  are computed, respectively. Some illustration for the graphs of the exact and approximate solutions are depicted in Figure 11.

**Table 3.** The errors  $e_n$  of Example 7 for five different quasi-affine tight framelet systems generated by the UEP and OEP, for increasing  $n$ .

$n$	HAAR Framelet	$B_2$ -UEP	$B_4$ -UEP	$B_2$ -OEP	$B_4$ -OEP
2	$6.47 \times 10^{-2}$	$1.04 \times 10^{-3}$	$6.07 \times 10^{-7}$	$1.03 \times 10^{-3}$	$4.45 \times 10^{-7}$
3	$3.23 \times 10^{-2}$	$4.73 \times 10^{-4}$	$8.33 \times 10^{-8}$	$1.08 \times 10^{-4}$	$1.78 \times 10^{-7}$
4	$2.68 \times 10^{-2}$	$8.76 \times 10^{-4}$	$3.35 \times 10^{-8}$	$1.25 \times 10^{-4}$	$4.35 \times 10^{-8}$
5	$1.76 \times 10^{-3}$	$1.56 \times 10^{-5}$	$1.25 \times 10^{-8}$	$9.78 \times 10^{-5}$	$1.58 \times 10^{-9}$
6	$2.11 \times 10^{-4}$	$1.05 \times 10^{-5}$	$4.33 \times 10^{-9}$	$3.45 \times 10^{-6}$	$6.92 \times 10^{-11}$
7	$7.93 \times 10^{-5}$	$6.84 \times 10^{-6}$	$5.53 \times 10^{-10}$	$2.39 \times 10^{-6}$	$5.92 \times 10^{-11}$
8	$9.02 \times 10^{-5}$	$5.56 \times 10^{-6}$	$5.51 \times 10^{-11}$	$5.98 \times 10^{-7}$	$1.82 \times 10^{-13}$
9	$2.50 \times 10^{-6}$	$1.98 \times 10^{-7}$	$1.02 \times 10^{-12}$	$5.45 \times 10^{-8}$	$3.11 \times 10^{-14}$
10	$4.05 \times 10^{-7}$	$2.34 \times 10^{-8}$	$2.42 \times 10^{-13}$	$2.12 \times 10^{-9}$	$4.23 \times 10^{-15}$

**Table 4.** Numerical results of the function  $u_n$  of Example 7 using different quasi-affine tight framelets and for a level of  $n = 2$ .

$x$	Exact	HAAR Framelet	$B_2$ -UEP	$B_4$ -UEP	$B_2$ -OEP	$B_4$ -OEP
0.0	1.00000000	1.07061012	0.99866232	0.99999601	0.99863491	0.999999958
0.1	1.10517092	1.09061851	1.10508652	1.10517150	1.10505007	1.105170028
0.2	1.22140276	1.21247432	1.22209321	1.22140205	1.22203402	1.221402071
0.3	1.34985880	1.37321902	1.35065092	1.34985878	1.35060677	1.349858253
0.4	1.49182470	1.55532117	1.49179223	1.49182450	1.49179044	1.491824418
0.5	1.64872127	1.76165283	1.64658432	1.64872193	1.64660927	1.648721644
0.6	1.82211880	1.80165032	1.82197332	1.82211894	1.82198698	1.822118840
0.7	2.01375270	2.01543677	2.01488843	2.01375233	2.01490121	2.013752248
0.8	2.22554090	2.26031276	2.22684809	2.22554035	2.22686599	2.225540081
0.9	2.45960311	2.46041532	2.45955456	2.45960353	2.45956180	2.459603410
1.0	2.71828180	2.72765982	2.71485007	2.71828155	2.71483561	2.718281710

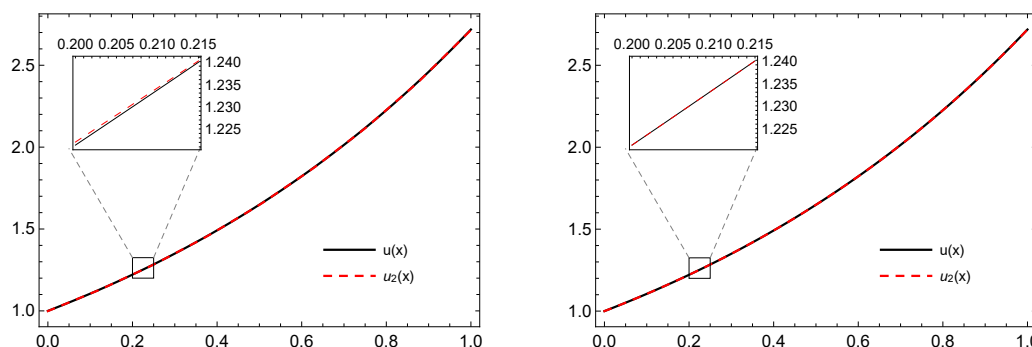


**Figure 11.** The graphs of  $u$  and  $u_n$  for  $n = 2$ , based on the quasi-affine  $B_2$ -UEP and  $B_4$ -UEP framelet systems, respectively, of Example 7.

To see the convergence of the proposed method using the quasi-affine tight framelet systems, we use the log-log scale plot. Then, it is clear that as the partial sum increases, the error between the approximated solution and exact solution approaches zero. The error history (log-log scale plot) of Examples 6 and 7 is displayed in Figure 12, where we see very accurate convergence rates too. This confirmed with respect to the theoretical predictions in the error analysis.

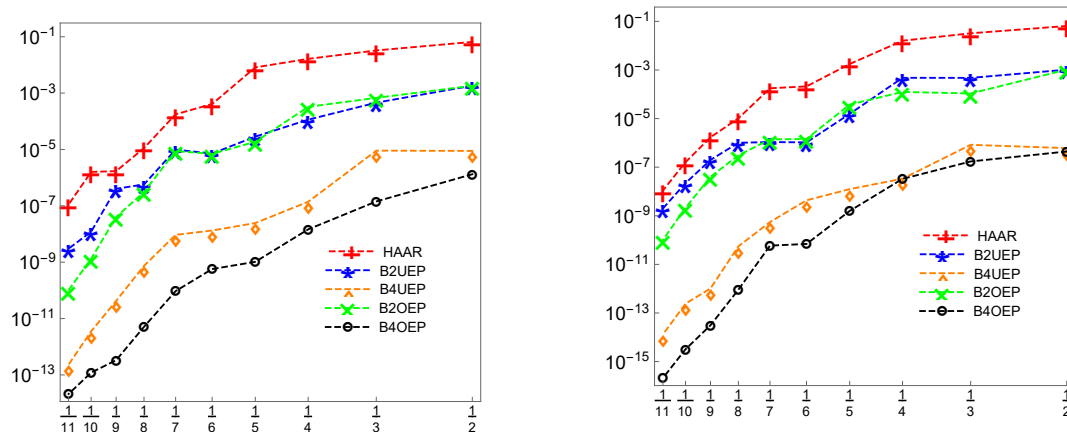


**Figure 12.** The convergence rate graph of Examples 6 and 7 given in the log-log scale plot, respectively.

## 7. Conclusions

We created a new, efficient method for solving Fredholm integral equations of the second kind. It turns out our method is efficient and has great accuracy. The proposed method shows highly accurate results and the performance of the present method is reliable, efficient and converges to the exact solution. Furthermore, the accuracy improves with increasing the partial sums and the number of vanishing moments of the  $B$ -splines quasi-affine tight framelets generated using the UEP and OEP.

**Funding:** This research was funded by Zayed University Research Fund.

**Acknowledgments:** The author would like to thank the anonymous reviewers for their valuable comments to improve the quality of the paper.

**Conflicts of Interest:** The author declare no conflict of interest.

## References

1. Ionescu, M.; Okoudjou, K.A.; Rogers, L.G. Some spectral properties of pseudo-differential operators on the Sierpinski gasket. *Proc. Am. Math. Soc.* **2017**, *145*, 2183–2198. [CrossRef]
2. Daubechies, I. *Ten Lectures on Wavelets*; SIAM: Philadelphia, PA, USA, 1992.
3. Grochenig, K. *Foundations of Time-Frequency Analysis*; Birkhäuser: Boston, MA, USA, 2001.
4. Han, B. Framelets and wavelets: Algorithms, analysis, and applications. In *Applied and Numerical Harmonic Analysis*; Birkhäuser/Springer: Cham, Switzerland, 2017.
5. Mallat, S.G. *A Wavelet Tour of Signal Processing*, 2nd ed.; Elsevier: Amsterdam, The Netherlands, 1999.
6. Meyer, Y. *Wavelets and Operators*; Cambridge University Press: Cambridge, UK, 1992.
7. Meyer, Y. Oscillating Patterns in Image Processing and Nonlinear Evolution Equations: The Fifteenth Dean Jacqueline B. Lewis Memorial Lectures. American Mathematical Society. Available online: <https://bookstore.ams.org/ulect-22> (accessed on 21 May 2019).
8. Duffin, R.; Schaeffer, A. A class of nonharmonic Fourier series. *Trans. Am. Math. Soc.* **1952**, *72*, 341–366. [CrossRef]
9. Adeg, Z.; Heydari, M.; Loghman, G.B. Numerical solution of Fredholm integral equations of the second kind by using integral mean value theorem. *Appl. Math. Model.* **2011**, *35*, 2374–2383.
10. Lepik, U.; Tamme, E. Application of the Haar wavelets for solution of linear integral equations. In Proceedings of the Dynamical Systems and Applications, Antalya, Turkey, 5–10 July 2005; pp. 395–407.
11. Singh, B.; Bhardwaj, A.; Alib, R. A wavelet method for solving singular integral equation of MHD. *Appl. Math. Comput.* **2009**, *214*, 271–279 [CrossRef]
12. Islam, M.S.; Shirin, A. Numerical Solutions of Fredholm Integral Equations of Second Kind Using Piecewise Bernoulli Polynomials. *Dhaka Univ. J. Sci.* **2011**, *59*, 103–107.
13. Cai, J.; Dong, B.; Shen, Z. Image restorations: A wavelet frame based model for piecewise smooth functions and beyond. *Appl. Comput. Harm. Anal.* **2016**, *41*, 94–138. [CrossRef]

14. Shen, Y.; Han, B.; Braverman, E. Adaptive frame-based color image denoising. *Appl. Comput. Harm. Anal.* **2016**, *41*, 54–74. [[CrossRef](#)]
15. Yang, J.; Zhu, G.; Tong, D.; Lu, L.; Shen, Z. B-spline tight frame based force matching method. *J. Comput. Phys.* **2018**, *362*, 208–219. [[CrossRef](#)]
16. Young, R. *An Introduction to Non-Harmonic Fourier Series*; Academic Press: New York, NY, USA, 1980.
17. Daubechies, I.; Grossmann, A.; Meyer, Y. Painless nonorthogonal expansions. *J. Math. Phys.* **1986**, *341*, 1271–1283. [[CrossRef](#)]
18. Ron, A. Factorization theorems of univariate splines on regular grids. *Isr. J. Math.* **1990**, *70*, 48–68. [[CrossRef](#)]
19. Chui, C.K.; He, W.; Stockler, J. Compactly supported tight and sibling frames with maximum vanishing moments. *Appl. Comput. Harmon. Anal.* **2002**, *341*, 224–262. [[CrossRef](#)]
20. Daubechies, I.; Han, B.; Ron, A.; Shen, Z. Framelets: MRA-based constructions of wavelet frames. *Appl. Comput. Harmon.* **2003**, *14*, 1–46. [[CrossRef](#)]
21. Ron, A.; Shen, Z. Affine systems in  $L^2(\mathbb{R}^d)$  II: Dual systems. *J. Fourier Anal. Appl.* **1997**, *3*, 617–637. [[CrossRef](#)]
22. Ron, A.; Shen, Z. Affine systems in  $L^2(\mathbb{R}^d)$ : The analysis of the analysis operators. *J. Funct. Anal.* **1997**, *148*, 408–447. [[CrossRef](#)]
23. Mohammad, M.; Lin, E. Gibbs Phenomenon in Tight Framelet Expansions. *Commun. Nonlinear Sci. Numer. Simul.* **2018**, *55*, 84–92. [[CrossRef](#)]
24. Mohammad, M.; Lin, E. Gibbs effects using Daubechies and Coiflet tight framelet systems, Frames and Harmonic Analysis. *Contemp. Math.* **2018**, *706*, 271–282.
25. Atindehou, A.G.D.; Kouagou, Y.B.; Okoudjou, K.A. Frame sets for generalized B-splines. *arXiv* **2018**, arXiv:1804.02450.
26. He, T. Eulerian polynomials and B-splines. *J. Comput. Appl. Math.* **2012**, *236*, 3763–3773. [[CrossRef](#)]
27. De Boor, C. *A Practical Guide to Splines*; Springer: New York, NY, USA, 1978.
28. Dong, B.; Shen, Z. MRA Based Wavelet Frames and Applications. 2010. Available online: <ftp://ftp.math.ucla.edu/pub/camreport/cam10-69.pdf> (accessed on 21 May 2019).
29. Bhatti, M.I.; Bracken, P. Solutions of differential equations in a Bernstein polynomial basis. *J. Comput. Appl. Math.* **2007**, *205*, 272–280. [[CrossRef](#)]
30. Liang, X.Z.; Liu, M.C.; Che, X.J. Solving second kind integral equations by Galerkin methods with continuous orthogonal wavelets. *J. Comput. Appl. Math.* **2001**, *136*, 149–161. [[CrossRef](#)]
31. De Boor, C.; DeVore, R.; Ron, A. Approximation from shift-invariant subspaces of  $L^2(\mathbb{R}^d)$ . *Trans. Am. Math. Soc.* **1994**, *341*, 787–806.
32. Borup, L.; Gribonval, R.; Nielsen, M. Bi-framelet systems with few vanishing moments characterize Besov spaces. *Appl. Comput. Harmon. Anal.* **2004**, *17*, 3–28. [[CrossRef](#)]

